Electromagnetically induced transparency in a thin vapor film

David Petrosyan[1,2] and Yu. P. Malakyan[1]
[1]*Institute for Physical Research, Armenian National Academy of Sciences, Ashtarak-2, 378410, Armenia*
[2]*Foundation for Research and Technology–Hellas, Institute of Electronic Structure and Laser, P.O. Box 1527, Heraklion 71110, Crete, Greece*
(Received 19 November 1999; published 18 April 2000)

We examine the effect of electromagnetically induced transparency in a thin cell filled with a vapor of three-level Λ atoms. We show that the absorption spectrum of the probe field and the fluorescence signal from the upper atomic level contain two sub-Doppler dips that have considerably different widths. The narrow dip corresponds to the effect of electromagnetically induced transparency, whereas the broader one results from the optical pumping of the external atomic states. Under the condition of exact resonance of the coupling field with the corresponding atomic transition, these two dips are superimposed on the frequency scale, while in the case of nonzero detuning of the coupling field, the two dips are shifted with respect to each other, which makes it possible to observe a competition between the two effects. In the frequency region where the absorption is low, large optical nonlinearities conditioned merely by the slow atoms having an effective 1 mK temperature are also found.

PACS number(s): 42.50.Gy, 32.80.−t, 42.62.Fi

I. INTRODUCTION

The effect of electromagnetically induced transparency (EIT) [1] has attracted much interest as a basic mechanism for a number of novel optical phenomena such as lasing without population inversion [2,3], pulse matching [4], enhanced index of refraction [5], or resonantly enhanced nonlinear processes [6]. The essence of EIT is a phenomenon of coherent population trapping (CPT) [7] in which the application of two laser fields to a three-level atomic system creates a specific coherent superposition of the atomic states—the so-called ''dark state''— which is stable against absorption of both fields. Experimentally, the steady-state EIT has been widely studied in usual vapor cells, where the thermal atomic motion, as a rule, tends to average the contribution of various atoms having different velocities and corresponding time of flight and collisional broadening of the atomic coherences, effectively smearing out the fine structure of the absorption and dispersion profiles. Meanwhile, the combination of the EIT and the newly developed technology of cooling and trapping atoms does not contain such a disadvantage, which made it possible to achieve recently an extreme reduction of light group velocity up to $10^{-7}c$ [8]. However, another recent report [9] has demonstrated that, under the condition of copropagating laser fields and with a proper choice of experimental parameters, the same order of magnitude for the light group velocity is achievable even in a usual vapor cell.

This paper is devoted to the study of the EIT effect in a vapor of three-level Λ atoms confined in an ultrathin cell with a thickness of only a few μm. In this cell, for low enough atomic density, the time of uninterrupted interaction of atoms with electromagnetic fields eventually coincides with the velocity-dependent wall-to-wall transit time of the atoms. On the other hand, the CPT time is of the order of $\Gamma(\Omega_c^2+\Omega_p^2)^{-1}$, where Γ is the half-width of the resonant with the probe field atomic transition, and Ω_c and Ω_p are the Rabi frequencies of the coupling and probe fields, respectively [10,11]. Thus in a low power experiment with the light intensity of the order of 0.1–1 mW/cm^2, only the slowest atoms would have enough time to settle down into the dark state and, hence, the major contribution to the probe transparency peak and refractive index variation would come from these atoms. At the same time, the fast atoms absorb the probe field only linearly during their wall-to-wall time of flight. This leads to the fact that in a thin film the probe absorption never vanishes, in contrast to the usual thermal vapor cell, where a Doppler-free EIT window has, in principle, vanishing absorption at the line center [1].

Our motivation for the present work is also related to the possible narrowing of the linewidth of the probe transparency peak down to the natural limit. For Λ atoms, the relevant parameter is the damping rate of the coherence between the ground states that is responsible for the trapping effect [7]. Many experimental parameters determine the observed linewidth of the transparency peak, e.g., amplitude and frequency fluctuations of the laser fields, atomic collisional broadening, influence of external fields, and time-of-flight broadening. The latter, being a phenomenological constant, is usually introduced into the theoretical calculations on CPT as a parameter to fit the experimental data [11,12]. In the case of a thin vapor cell, however, it is possible to take into account the finite interaction time exactly without introducing any unknown parameter. This procedure is described in the following section and it requires that the coherence between the atomic ground states does not survive (even partially) during atom-wall collisions. This is the main assumption we have made in this work. Another interesting aspect is the possibility of observing a competition between the CPT and the optical pumping (OP). In practice it is very difficult to find a closed Λ system since, as a rule, there always exist some ground-state sublevels that are not excited by the applied fields and, in the mean time, the atomic population decays to these ''external'' states. Actually, the CPT is always accompanied by the OP. Indirect evidence of the influence of OP on the formation and properties of the dark state

has been recently obtained in the experiments with a thermal sodium beam [13] by measuring the time-averaged fluorescence signal. The fact that the OP alone originates a sub-Doppler structure in the transmission spectrum of an open atomic system was theoretically predicted in [14,15] and experimentally observed in an ultrathin cell with a single light beam in [16]. In the present paper we show that in a thin vapor film the absorption spectrum of the normal incident to the cell probe field and the fluorescence signal from the upper atomic level contain two sub-Doppler dips that correspond to the effects of OP and EIT. By choosing different detunings of the coupling field from the respective atomic transition resonance, it is possible to separate the contribution of the two effects.

The paper is organized as follows. In the next section we derive equations for the time evolution of the atomic density matrix and for the field transmitted through the cell. On the basis of the mathematical formalism obtained there, we present in Sec. III the results of numerical calculations performed for a realistic experimental setup. Our conclusions are summarized in Sec. IV. Finally, in the Appendix we obtain analytic results on EIT for a special case of exact resonances of both fields with the corresponding atomic transitions.

II. FORMULATION

We consider a stationary interaction of two copropagating electromagnetic fields with a vapor of three-level Λ atoms confined in an ultrathin cell of thickness L. The density of atoms N is assumed to be low enough so that the time of free flight of the atoms having a mean thermal velocity $\langle v\rangle$ largely exceeds the time $\tau=L/\langle v\rangle$ of the atomic flight between two walls of the cell. Throughout the present work it is also assumed that the atoms experience inelastic collisions with the cell walls during which they lose optical excitation and all memory about the previous state. Having made these two assumption, we can avoid using in our treatment a phenomenological constant responsible for the collisional relaxations of atomic excitation and coherences and take these effects into account exactly by solving the temporal equations governing the evolution of the atomic density matrix with proper boundary conditions for each atom separately, as described below.

A. Model atomic system

The atomic system is depicted in Fig. 1, where the unperturbed atomic levels $|1\rangle$, $|2\rangle$, and $|3\rangle$ have energies $\hbar\omega_1$, $\hbar\omega_2$, and $\hbar\omega_3$, respectively. The atom interacts with two electric fields $E_{c,p}$ having the frequencies $\omega_{c,p}$ and working on the transitions $|1\rangle\rightarrow|3\rangle$ and $|2\rangle\rightarrow|3\rangle$, respectively. These fields are detuned from the atomic resonances by the detunings

$$\Delta_c=\omega_{31}-\omega_c, \quad \Delta_p=\Delta_c-\delta_R=\omega_{32}-\omega_p, \tag{1}$$

where ω_{ik} is the energy difference between the levels i and k, and

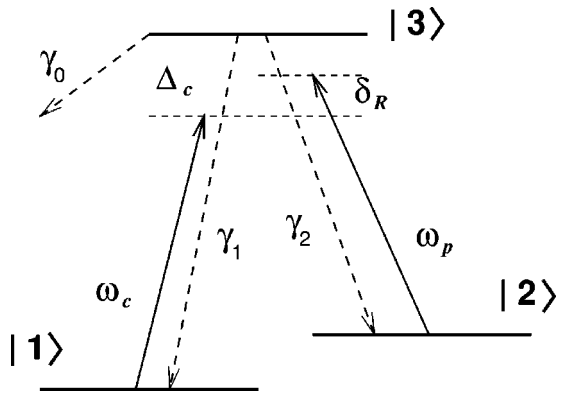

FIG. 1. Schematic representation of the atomic system.

$$\delta_R=\omega_{21}+\omega_p-\omega_c \tag{2}$$

is the two-photon Raman detuning on the transition $|1\rangle\rightarrow|2\rangle$. In the dipole approximation, the total interaction picture Hamiltonian corresponding to this system can be written as

$$H_{\rm int}=\hbar\delta_R|2\rangle\langle 2|+\hbar\Delta_c|3\rangle\langle 3| -\hbar(\Omega_c|3\rangle\langle 1|+\Omega_p|3\rangle\langle 2|+\text{H.c.}). \tag{3}$$

Here the Rabi frequencies of the corresponding fields are defined as $\Omega_c=\mu_{13}E_c/2\hbar$ and $\Omega_p=\mu_{23}E_p/2\hbar$, where μ_{ik} is the dipole matrix element of the transition $i\rightarrow k$ which can be expressed through the radiative decay rate $\gamma_{k\rightarrow i}$ as

$$|\mu_{ik}|^2=\frac{3\hbar c^3}{4\omega_{ki}^3}\gamma_{k\rightarrow i}.$$

The time evolution of the system's density matrix ρ obeys the master equation

$$\frac{d}{dt}\rho=-\frac{i}{\hbar}[H_{\rm int},\rho]+\Lambda\rho. \tag{4}$$

In our model, the longitudinal and transverse relaxations of the atomic Bloch vectors are determined only by the process of spontaneous emission from the upper level $|3\rangle$ to the lower levels $|1\rangle$ and $|2\rangle$ and outside of the three-level system. According to the assumptions made in the beginning of this section, the time of free flight of an atom having the velocity v along the cell axis z is solely determined by the time interval between two subsequent collisions with the cell walls, due to which the atom loses optical excitation and then departs from the surface having equal populations of the lower levels $|1\rangle$ and $|2\rangle$. As such, the phenomenological relaxation matrix $\Lambda\rho$ has a form

$$\Lambda\rho=\begin{pmatrix}\gamma_1\rho_{33} & 0 & -\Gamma\rho_{13}\\ 0 & \gamma_2\rho_{33} & -\Gamma\rho_{23}\\ -\Gamma\rho_{31} & -\Gamma\rho_{32} & -2\Gamma\rho_{33}\end{pmatrix}, \tag{5}$$

where $2\Gamma=\gamma_0+\gamma_1+\gamma_2$ is the total spontaneous decay rate of the level $|3\rangle$, which is composed of the decays to the levels $|1\rangle$ and $|2\rangle$ with the rates γ_1 and γ_2, respectively, and the decay outside with the rate γ_0.

B. Probe absorption and phase shift

The spatial evolution of the probe field $E_p(z)$ along the z axis is determined by Maxwell's equation

$$\frac{d}{dz}E_p = i\frac{2\pi\omega_p}{c}P_p, \tag{6}$$

where P_p is the field induced polarization, real and imaginary parts of which are responsible for the dispersive and absorptive properties of the medium, respectively. For simplicity, we assume that the initial phases of both fields, E_p and E_c, are the same. For the probe field $E_p=|E_p|\exp(i\phi)$ written as a product of real amplitude $|E_p|$ and phase ϕ terms, Eq. (6) takes the form

$$\frac{d|E_p|}{dz} = -\frac{2\pi\omega_p}{c}\mathrm{Im}\left(\frac{P_p}{E_p}\right)|E_p| = -\frac{1}{2}\alpha|E_p|, \tag{7a}$$

$$\frac{d\phi}{dz} = \frac{2\pi\omega_p}{c}\mathrm{Re}\left(\frac{P_p}{E_p}\right) = \beta, \tag{7b}$$

where we have introduced the local absorption α and dispersion β coefficients of the medium on the frequency ω_p:

$$\alpha = \frac{4\pi\omega_p}{c}\mathrm{Im}\left(\frac{P_p}{E_p}\right), \tag{8a}$$

$$\beta = \frac{2\pi\omega_p}{c}\mathrm{Re}\left(\frac{P_p}{E_p}\right). \tag{8b}$$

The medium polarization P_p on this frequency is given by

$$P_p = 2N\mu_{23}[\rho_{32}^{+}+\rho_{32}^{-}], \tag{9}$$

where the nondiagonal matrix elements $\rho_{32}^{+}\equiv\rho_{32}(z=vt)$ and $\rho_{32}^{-}\equiv\rho_{32}(z=L-vt)$ relate to the atoms flying with the velocity $v(>0)$ in the positive and negative directions of the cell axis, respectively. Obviously, these two groups of atoms experience opposite Doppler shifts of the detunings of both fields from the atomic resonances:

$$\Delta_{c,p}^{\pm} = \Delta_{c,p} \pm \omega_{c,p}\frac{v}{c}.$$

Note, however, that for closely disposed lower levels $|1\rangle$ and $|2\rangle$ (e.g., hyperfine components of the same atomic state), the Raman detuning δ_R is practically the same for all atoms and is not affected by their thermal motion.

From Eq. (7a) for the intensity $I_p(z)\propto|E_p|^2$ of the probe at $z=L$ we obtain

$$I_p(L) = I_p(0)\exp\left(-\int_0^L\alpha(z)dz\right) \simeq I_p(0)\left(1-\int_0^L\alpha(z)dz\right). \tag{10}$$

In the last part of this equation we have replaced the exponent with its first-order Taylor expansion assuming, thus, that the absorption is weak. As we show in the next section, this simplification is well justified for a typical optical experiment with a thin cell [16]. Hence, for the relative absorption A and the phase shift of the probe at the exit from the cell, we obtain

$$A \equiv \frac{I_p(0)-I_p(L)}{I_p(0)} = \int_0^L\alpha(z)dz, \tag{11a}$$

$$\phi = \int_0^L\beta(z)dz. \tag{11b}$$

Next we need to take into account the atomic thermal motion which we assume to obey the Maxwellian distribution $W(v)=(u\sqrt{\pi})^{-1}\exp(-v^2/u^2)$ with u being the most probable velocity. Thus for the averaged over the atomic velocity distribution absorption $\langle A\rangle$ and phase shift $\langle\phi\rangle$ we obtain finally the following equations:

$$\langle A\rangle = \int_0^\infty W(v)dv\int_0^L\alpha(z)dz,$$

$$\langle\phi\rangle = \int_0^\infty W(v)dv\int_0^L\beta(z)dz,$$

which in explicit form are given by

$$\langle A\rangle = A_0\int_0^\infty\exp(-v^2/u^2)v\,dv \times\int_0^{L/v}\mathrm{Im}\left[\frac{\rho_{32}^{+}(t,\Delta_{c,p}^{+})}{E_p}+\frac{\rho_{32}^{-}(t,\Delta_{c,p}^{-})}{E_p}\right]dt, \tag{12a}$$

$$\langle\phi\rangle = \frac{A_0}{2}\int_0^\infty\exp(-v^2/u^2)v\,dv \times\int_0^{L/v}\mathrm{Re}\left[\frac{\rho_{32}^{+}(t,\Delta_{c,p}^{+})}{E_p}+\frac{\rho_{32}^{-}(t,\Delta_{c,p}^{-})}{E_p}\right]dt, \tag{12b}$$

where the coefficient

$$A_0 = \frac{8N\sqrt{\pi}\omega_p\mu_{23}}{uc}.$$

In Eqs. (12) the integration over the spatial coordinate z has been replaced by the integration over the time $0\leqslant t\leqslant\tau$ ($\tau=L/v$) of free interaction of atoms with both fields: $\int_0^L dz\rightarrow v\int_0^{L/v}dt$.

Another quantity that we use in Sec. III and that is proportional to the fluorescence signal from the excited atoms is the upper level population ρ_{33}. Following the same reasoning as in the derivation of Eqs. (12), for the space integrated and velocity averaged population $\langle\rho_{33}\rangle$ of the upper state of the atoms in the cell we obtain

$$\langle \rho_{33} \rangle = \frac{1}{\sqrt{\pi} u L} \int_0^\infty \exp(-v^2/u^2) v\, dv \times \int_0^{L/v} [\rho_{33}^+(t, \Delta_{c,p}^+) + \rho_{33}^-(t, \Delta_{c,p}^-)] dt, \quad (13)$$

where $\rho_{33}^+ \equiv \rho_{33}(z = vt)$ and $\rho_{33}^- \equiv \rho_{33}(z = L - vt)$.

To get an idea about contributions to the absorption by the atoms with various velocities, we define also a velocity-dependent partial absorption

$$A_{\text{part}}(v) = \frac{A_0}{\langle A \rangle} \int_0^v \exp(-v'^2/u^2) v'\, dv' \times \int_0^{L/v'} \text{Im}\left[\frac{\rho_{32}^+(t, \Delta_{c,p}^+)}{E_p} + \frac{\rho_{32}^-(t, \Delta_{c,p}^-)}{E_p} \right] dt, \quad (14)$$

which is normalized by the total absorption $\langle A \rangle$.

Equations. (12), (13), and (14) are the central equations of this paper. In these equations, for each group of atoms having the velocity v, the density-matrix elements are found by (numerical) integration of the master equation (4) with the initial conditions $\rho_{11}(0) = \rho_{22}(0) = \frac{1}{2}, \rho_{33}(0) = \rho_{ik}(0) = 0$ $(i \neq k)$.

The delay time T_{del} of the E_p field after passing through the cell, relative to the time T_{vac} of passing through the vacuum, is given by [8]

$$T_{\text{del}}(\omega_p) = \frac{d\langle \phi \rangle}{d\omega_p}. \quad (15)$$

In the frequency region where $T_{\text{del}}(\omega_p)$ is approximately constant and much larger than T_{vac}, for the group velocity V_{group} of the probe we have

$$V_{\text{group}} = \frac{L}{T_{\text{del}} + T_{\text{vac}}} \simeq L \left(\frac{d\langle \phi \rangle}{d\omega_p} \right)^{-1}. \quad (16)$$

Thus in the frequency region where the derivative $(d\langle \phi \rangle / d\omega_p)$ takes a large positive value, the reduction of the group velocity of the probe field is significant.

III. NUMERICAL RESULTS AND DISCUSSION

Here we present the results of numerical calculations based on the equations derived in the preceding section and give the discussion of relevant physics.

In our simulations for the model atomic system we have chosen parameters corresponding to the D_1 line of ^{23}Na. The most probable velocity of the atoms $u = 460$ m/s at room temperature $T = 20°\text{C}$, for which, with $\omega_{p,c} \simeq 2\pi\ 5.083 \times 10^{14}$ rad/s, the inhomogeneous Doppler broadening width is equal to 955 MHz. The total decay rate of the upper level $|3\rangle$, corresponding to the state $3P_{1/2}$ $(F = 2)$ of Na, is $2\Gamma = 6.277 \times 10^7$ s^{-1}. The lower atomic levels $|1\rangle$ and $|2\rangle$ correspond to the hyperfine components $F = 1$ and $F = 2$ of the ground state $3S_{1/2}$, respectively. The separation of these levels $\omega_{21}/2\pi = 1772$ MHz is almost twice as large as the Doppler width. The separation of the two hyperfine components, $F = 1$ and $F = 2$, of the upper state $3P_{1/2}$ is, however, one order of magnitude smaller and, hence, the inhomogeneous broadening well overlaps these two states. In our model, we do not take into account the second upper level having in mind that, in principle, one can incorporate into the present treatment the hyperfine splitting of the excited atomic state. At the end of this section we make, however, some predictions on the behavior of the nonidealized system which are based on a simple physical reasoning. The decay 2Γ is composed of $\gamma_1 = 2.574 \times 10^7$ s^{-1}, $\gamma_2 = 1.381 \times 10^7$ s^{-1}, and $\gamma_0 = 2.323 \times 10^7$ s^{-1}. The latter represents the population leak from the level $|3\rangle$ towards those magnetic substates of the atom that do not form a Λ system in the presence of the two applied fields—the process that is responsible for the OP. For the cell length $L = 10$ μm the density of atoms N is taken to be rather low $(N = 5 \times 10^{12}$ cm$^{-3})$ in order not to violate the assumption made in the preceding section.

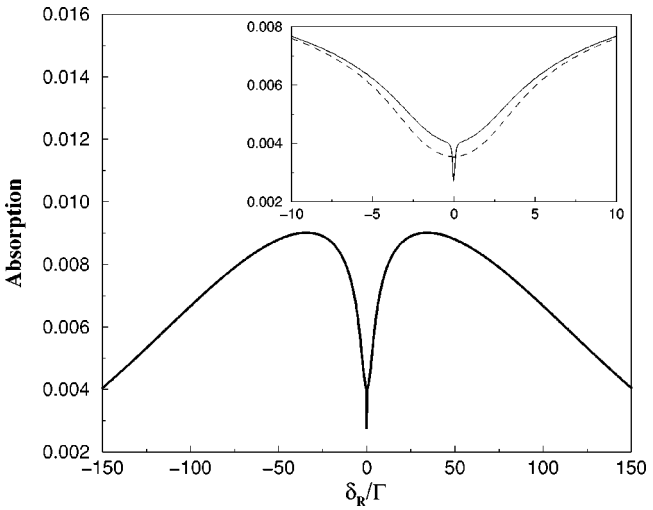

FIG. 2. Probe absorption $\langle A \rangle$ [see Eq. (12a)] as a function of the Raman detuning δ_R (normalized by Γ) for the case $\Delta_c = 0$ and $\Omega_c = \Omega_p = 0.3\Gamma$. Inset: a zoom of the same graph in the vicinity of $\delta_R = 0$; the dashed line is the pure OP curve when $\Omega_c = 0$. Other parameters are given in the text (Sec. III).

In Fig. 2 we plot the probe absorption calculated from Eq. (12a) as a function of the Raman detuning δ_R for the case $\Delta_c = 0$ and $\Omega_c = \Omega_p = 0.3\Gamma$ $(I_p = 5 \times 10^{-3}\text{W/cm}^2)$. For the same set of parameters we plot in Fig. 3 the upper level population $\langle \rho_{33} \rangle$ which is proportional to the fluorescence signal from that level. One can see a sub-Doppler absorption (and fluorescence) dip consisting of two superimposed Lorentzians, the first of which—the broader one—represents the absorption reduction due to the OP of the external levels of the Λ atom with the rate γ_0, while the second much narrower dip is due to the EIT effect. A comprehensive introduction of EIT in terms of the system's noncoupled (dark) and coupled states is given in the Appendix. For comparison we plot on the same graphs the pure contribution of the OP in the absence of the coupling field $\Omega_c = 0$. In an ultrathin cell the absorption reduction of the probe in the vicinity of the atomic line center results from the fact that only the

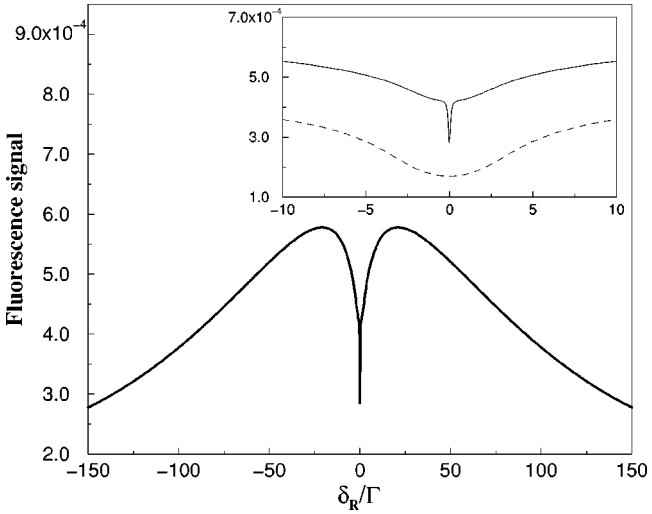

FIG. 3. Fluorescence signal $\langle \rho_{33} \rangle$ from the upper level $|3\rangle$ [see Eq. (13)] as a function of the Raman detuning δ_R for the same set of parameters as in Fig. 2. Inset: a zoom of the same graph; the dashed line is the pure OP curve when $\Omega_c = 0$.

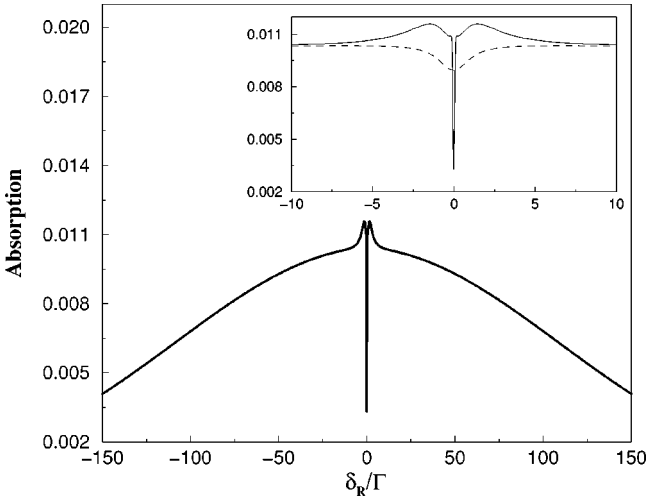

FIG. 4. Probe absorption $\langle A \rangle$ as a function of the Raman detuning δ_R for the case $\Delta_c = 0$, $\Omega_c = 0.3\Gamma$, and $\Omega_p = 0.03\Gamma$. Inset: a zoom of the same graph; the dashed line is the pure OP curve when $\Omega_c = 0$.

slowest atoms have enough time to undergo a complete OP [14–16]. For moderate laser field intensities, the efficiency η of OP per unit time is proportional to the ratio of the Rabi frequency of the field to its detuning from the atomic resonance:

$$\eta \simeq \frac{\Omega_p^2}{\Delta_p^{\pm 2} + \Gamma^2} \gamma_0, \tag{17}$$

where the detuning $\Delta_p^{\pm}$ includes also the Doppler shift. Thus, while scanning the probe laser, those atoms that have detunings $|\Delta_p^{\pm}| > \Gamma$ interact with the field weakly and give only a linear contribution to the absorption and fluorescence during their wall-to-wall time of flight. Some of the atoms having the corresponding Doppler shift compensate for the probe detuning ($\Delta_p^{\pm} \simeq 0$), but due to the nonvanishing velocity component along the z axis, they also do not have enough time for a complete OP. Only the slowest atoms, when the laser is tuned into resonance with the atomic transition, simultaneously have vanishing detuning and enough time to undergo a complete OP. On the other hand, when the coupling field E_c is on, the OP of the lower level $|1\rangle$ becomes reversible, which causes the increase of the probe absorption and the fluorescence signal (see Figs. 2 and 3), since the latter is proportional to Ω_c^2 as follows from Eq. (A2c) of the Appendix. At the same time, we observe a superimposed narrow EIT dip. Similarly to the OP effect, for the CPT in the lower levels $|1\rangle$ and $|2\rangle$ to settle down, enough interaction time [of the order of $\Gamma(\Omega_c^2 + \Omega_p^2)^{-1}$] is needed. Therefore, only the slowest atoms are trapped in the dark state and do not contribute to the absorption. The narrow width of the EIT dip in comparison with the OP dip can be understood if we recall the fact that the EIT effect takes place only in the frequency region where the Raman resonance condition $\delta_R = 0$ is satisfied with an accuracy $|\delta_R| < \gamma_{12}$ [7], where γ_{12} is the rate of relaxation of the coherence between the levels $|1\rangle$ and $|2\rangle$. In our model this relaxation results from the atomic collisions with the cell walls. Since only the slowest atoms are responsible for the EIT effect, the ground levels' coherence relaxation time for these atoms is very large and we observe an extremely narrow EIT dip. Note further that in Figs. 2 and 3 the absorption and fluorescence do not vanish even at the line center since, as mentioned above, the fast atoms absorb the probe field linearly during their wall-to-wall time of flight.

In Figs. 4 and 5 we plot the probe absorption and the fluorescence signal for the case $\Omega_p = 0.03\Gamma$ ($I_p = 5 \times 10^{-5}$W/cm^2), i.e., the Rabi frequency of the probe field E_p is reduced 10 times. We see that, in accordance with Eq. (17), for this magnitude of Ω_p the effect of OP is reduced

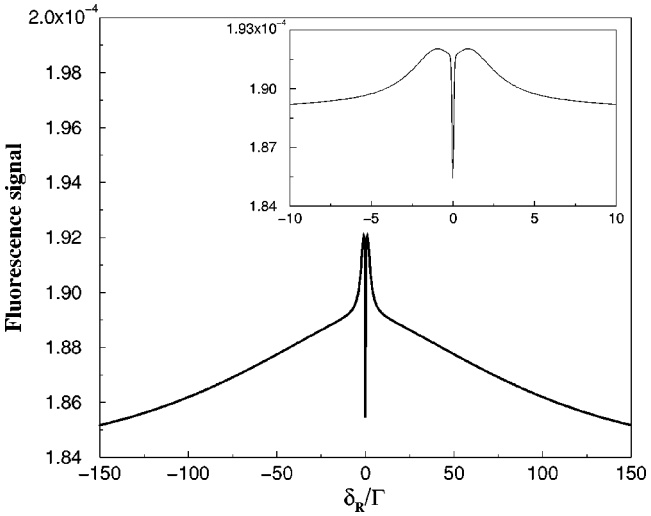

FIG. 5. Fluorescence signal $\langle \rho_{33} \rangle$ from the upper level $|3\rangle$ as a function of the Raman detuning δ_R for the same set of parameters as in Fig. 4. Inset: a zoom of the same graph.

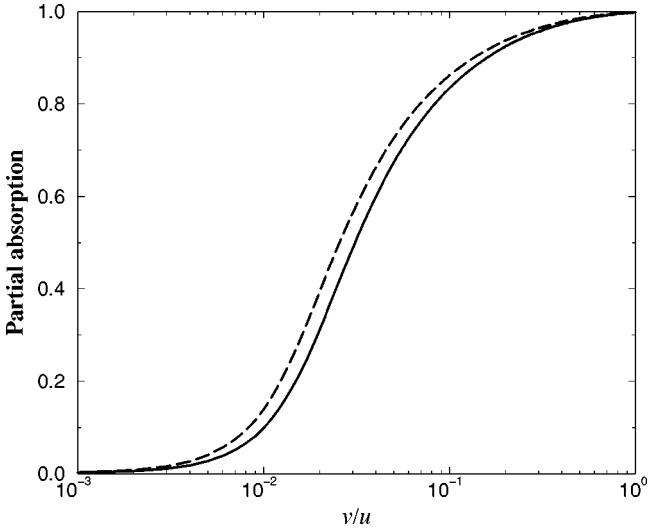

FIG. 6. Partial absorption of the probe A_{part} [see Eq. (14)] at $\delta_R=0$ as a function of the velocity of atoms v (normalized by u) for $\Delta_c=0$, $\Omega_c=0.3\Gamma$; $\Omega_p=0.3\Gamma$ (solid curve) and $\Omega_p=0.03\Gamma$ (dashed curve).

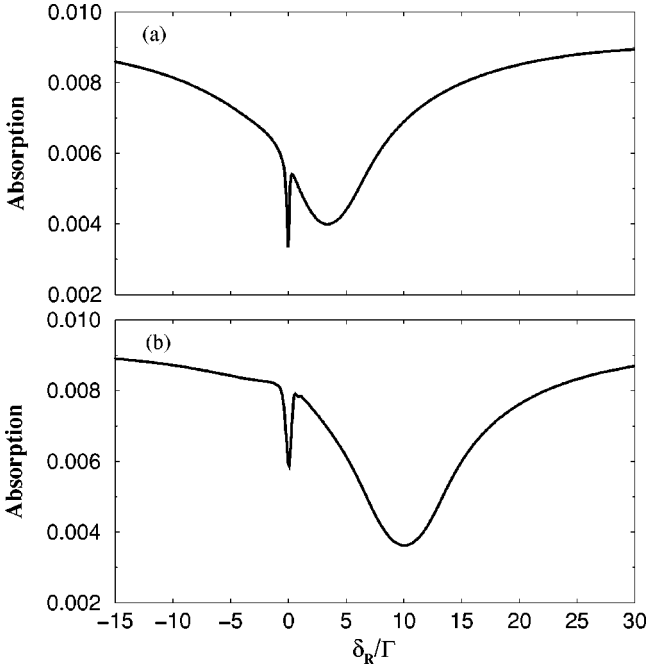

FIG. 7. Probe absorption $\langle A\rangle$ as a function of the Raman detuning δ_R for the case $\Omega_c=\Omega_p=0.3\Gamma$; $\Delta_c=3\Gamma$ (a) and $\Delta_c=10\Gamma$ (b).

significantly both in its width and depth. Note the increase of the absorption and fluorescence in the frequency regions adjacent to the EIT dip. This is due to the resonance of the probe field with the components of the Stark splitting of the upper level $|3\rangle$. In these figures, only the atoms with the thermal velocities $v\leqslant 0.002u$ (corresponding to a mK temperature) are trapped in the dark state and contribute to the EIT effect. To illustrate this fact, we show in the next figure the partial absorption of the probe at $\delta_R=0$ as a function of the velocity of atoms v calculated from Eq. (14). One can see that only relatively slow atoms, which have enough time to settle down into the dark state, do not participate in the absorption process. For a stronger probe field, less interaction time is needed for the atoms to be trapped. Therefore, the atoms with higher velocities become nonabsorbing, as is apparent from comparison of the two curves in Fig. 6.

Consider now the case of the finite detuning $\Delta_c\neq 0$ of the coupling field (Fig. 7). Here the absorption reduction of the probe field E_p due to the effects of OP and EIT takes place in the different frequency regions, which leads to the separation of the two Lorentzians. This is because for the EIT effect the Raman resonant condition $\delta_R=0$ is needed, while the effect of OP is most efficient in the vicinity of the resonance of the probe field with the atomic transition frequency.

We turn our attention now to the discussion of unusual dispersive properties of our system. The basic equation for this study is Eq. (12b), by means of which the delay time (15) and the corresponding group velocity of the probe (16) can be calculated. In Figs. 8 and 9 we present the phase shift of the probe at the exit from the cell as a function of the detuning δ_R. One can see in Fig. 8 that, similarly to the absorption spectra of Figs. 2 and 4, there are two superimposed dispersion curves, the first of which corresponds to the OP effect and the other (the steeper) one to the EIT. As discussed above, for the parameters corresponding to Fig. 8(b), the EIT effect results only from the slowest atoms ($v\leqslant 0.002u$), while faster atoms, due to the linear absorption, constitute a rather smooth background. Therefore, the averaging over the velocity distribution does not induce a significant spread of the dispersion curve. This leads to a fast variation of the dispersion in the vicinity of $\delta_R=0$ and, consequently, to a strong reduction of the group velocity of light. Thus in Fig. 8(b) for the delay time of the E_p field at

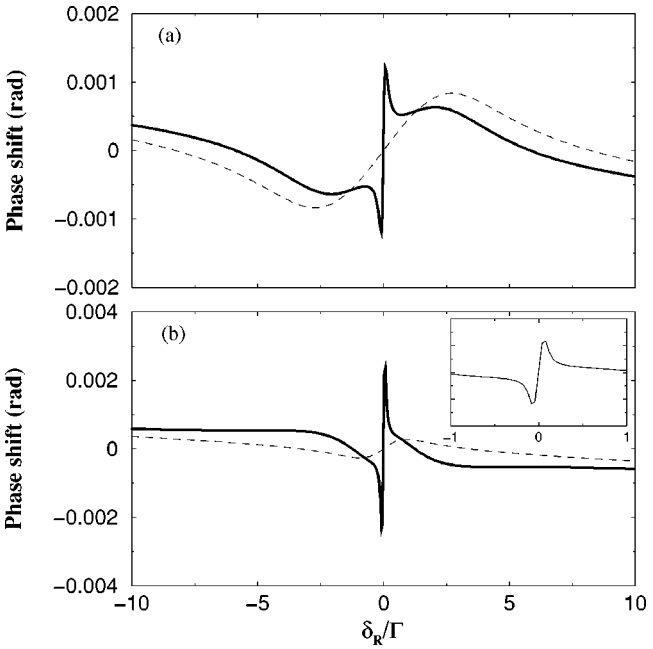

FIG. 8. Phase shift $\langle\phi\rangle$ of the field E_p at $z=L$ [see Eq. (12b)] as a function of the Raman detuning δ_R for the case $\Delta_c=0$, $\Omega_c=0.3\Gamma$; $\Omega_p=0.3\Gamma$ (a) and $\Omega_p=0.03\Gamma$ (b). The dashed lines are the pure OP curves when $\Omega_c=0$. Inset is a zoom of graph (b).

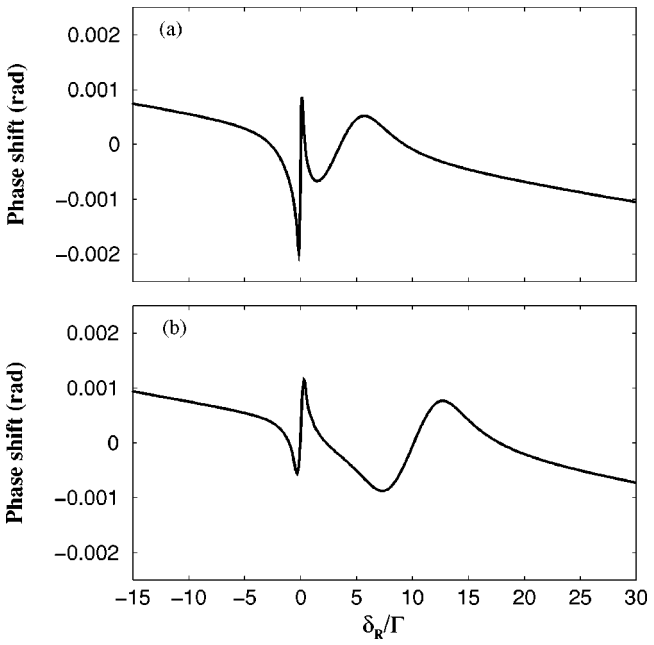

FIG. 9. Phase shift $\langle\phi\rangle$ of the field E_p at $z=L$ as a function of the Raman detuning δ_R for the case $\Omega_c=\Omega_p=0.3\Gamma$; $\Delta_c=3\Gamma$ (a) and $\Delta_c=10\Gamma$ (b).

the exit from the cell we have

$$T_{\mathrm{del}}=\frac{d\langle\phi\rangle}{d\omega_p}\Big|_{\delta_R=0}=1.8\times10^{-9}\ \ \mathrm{s},$$

which gives the group velocity as small as $V_{\mathrm{group}}\simeq1.8\times10^{-5}c$.

We have discussed so far a rather idealized model where the hyperfine splitting of the excited atomic state $3P_{1/2}$ was neglected. To proceed from the obtained results, we can foresee the appearance in a real experiment of the second OP dip on the absorption and fluorescence signal curves. Each of these dips would correspond to the probe field resonance with the atomic transition from the lower level $|2\rangle$ to the respective hyperfine sublevel of the excited state. The location of a single EIT dip, however, is independent of the presence of the second excited level and is always at $\delta_R=0$ on the Raman detuning scale.

IV. CONCLUSIONS

In conclusion, we have developed a formalism for rendering the (near) resonant interaction of two electromagnetic fields with an inhomogeneously broadened system consisting of three-level Λ atoms confined in an ultrathin cell of thickness 10 μm or less. The peculiar features of this model stem from the fact that the free interaction time of atoms with two laser fields is solely determined by the wall-to-wall time of atomic flight. Unusual absorptive and dispersive properties of this system have been found. Thus, we have shown that the absorption spectrum of the probe field and the fluorescence signal from the upper atomic level contain two sub-Doppler dips. One of them is originated from the OP due to the leak of atomic population from the upper level $|3\rangle$ while the other much narrower dip corresponds to the EIT effect established in the medium due to the CPT of the atoms in the lower levels $|1\rangle$ and $|2\rangle$. When the coupling field is tuned into the exact resonance with the atomic transition $|1\rangle\rightarrow|3\rangle$, the locations of the two dips on the frequency scale coincide, whereas in the case of nonzero detuning of the coupling field, the two dips are shifted from each other by the amount of this detuning. This is because the EIT effect is very sensitive to the Raman resonance condition $\delta_R=0$, while the effect of OP is most efficient in the vicinity of the resonance of the probe field with the atomic transition frequency.

Another interesting finding that has emerged from this study is a discovery of the unusual dispersive properties of this system in the frequency region where the absorption is low. The large optical nonlinearities are conditioned by those atoms that have a very small velocity component along the probe field propagation axis, therefore the averaging over the velocity distribution does not spread much the dispersion curve in the vicinity of $\delta_R=0$. In other words, the present scheme enables one to effectively separate the contribution of the ''cold'' superslow atoms. This gives an easy and robust recipe for obtaining a rather strong reduction of the speed of light with no need of using the expensive cold atom technology.

ACKNOWLEDGMENTS

This work has been supported by the Government of the Republic of Armenia (Scientific Project No. 96-770). We would like to thank Professor D. Sarkisyan for useful discussions.

APPENDIX

To discuss more quantitatively how the EIT is established under the conditions of the present scheme, we present here an analytic result for the special case $\Delta_p=\Delta_c=0$. Since we consider the probe and coupling field intensities to be below the saturation intensities of the corresponding atomic transitions, i.e. $\Omega_{p,c}<\Gamma$, in the time region $t>\Gamma^{-1}$ we can adiabatically eliminate the upper atomic level $|3\rangle$ and express the density-matrix elements ρ_{33},ρ_{31}, and ρ_{32} through the populations ρ_{11} and ρ_{22} of the lower levels and their coherence ρ_{21}. This will allow us to solve analytically the master equation (4) for the given initial conditions at $t=0$: $\rho_{11}(0)=R_1,\rho_{22}(0)=R_2=1-R_1$, and $\rho_{21}(0)=0$. It is convenient, however, to describe the evolution of the system in the basis of coupled $|C\rangle$ and noncoupled $|N\rangle$ states, defined as [7]

$$|C\rangle=\frac{\Omega_c}{\Omega}|1\rangle+\frac{\Omega_p}{\Omega}|2\rangle, \tag{A1a}$$

$$|N\rangle=\frac{\Omega_p}{\Omega}|1\rangle-\frac{\Omega_c}{\Omega}|2\rangle, \tag{A1b}$$

where $\Omega=\sqrt{\Omega_p^2+\Omega_c^2}$. As can be checked using the Hamiltonian (3), the noncoupled state is indeed decoupled from the

atomic state $|3\rangle$ and the coupled state $|C\rangle$. The density-matrix elements in the two bases are expressed through each other as

$$\rho_{CC}=(\Omega_c^2\rho_{11}+\Omega_p^2\rho_2 2+2\Omega_c\Omega_p \mathrm{Re}\rho_{21})/\Omega^2, \quad \text{(A2a)}$$

$$\rho_{NN}=(\Omega_p^2\rho_{11}+\Omega_c^2\rho_2 2-2\Omega_c\Omega_p \mathrm{Re}\rho_{21})/\Omega^2, \quad \text{(A2b)}$$

$$\rho_{33}\simeq\Omega^2\rho_{CC}/\Gamma^2. \quad \text{(A2c)}$$

The solution for the populations of the coupled and non-coupled states is given by

$$\rho_{CC}=R_C\exp(-\gamma t), \quad \text{(A3a)}$$

$$\rho_{NN}=R_N+\left(1-\frac{\Omega^2\gamma_0}{\Gamma^2\gamma}\right)R_C[1-\exp(-\gamma t)], \quad \text{(A3b)}$$

where

$$R_C=\rho_{CC}(0)=(\Omega_c^2R_1+\Omega_p^2R_2)/\Omega^2,$$

$$R_N=\rho_{NN}(0)=(\Omega_p^2R_1+\Omega_c^2R_2)/\Omega^2$$

are their initial values, and

$$\gamma=\frac{\Omega_p^2\gamma_1+\Omega_c^2\gamma_2}{\Gamma^2}+\frac{\Omega^2\gamma_0}{\Gamma^2} \quad \text{(A4)}$$

is the decay rate of the coupled state $|C\rangle$, which is composed of the decay to the noncoupled state $|N\rangle$ (first term) and the decay to the external states (second term) that is responsible for the OP. It is worth mentioning at this stage that in the case $\delta_R\neq 0$ the state $|N\rangle$ is not decoupled from the state $|C\rangle$ and the upper atomic level $|3\rangle$. Combining Eqs. (A2c) and (A3a) one can see that the fluorescence signal, being proportional to the population of the upper level $|3\rangle$, is most reduced in the line center where both terms of Eq. (A4) play an equally important role, while outside of the EIT window only the second term causes the reduction. Obviously this reduction originates only from the relatively slow atoms $v<L\gamma$ that have enough free interaction time. With regard to Eq. (A3b), some atoms having arbitrary velocities might initially be trapped in the noncoupled state, which is represented by the first term of this equation. Further increase of the population ρ_{NN} is, however, solely determined by slow atoms whose contribution is given by the second term of Eq. (A3b).

The equation for the probe absorption has a form

$$\alpha\propto\left\{R_2-\frac{\Omega^2(\Gamma-\gamma_2)}{\Gamma(\gamma\Gamma-\Omega^2)}R_C\left[1-\exp\left(-\frac{\gamma\Gamma-\Omega^2}{\Gamma}t\right)\right]\right\}$$
$$\times\exp\left(-\frac{\Omega^2}{\Gamma}t\right)+O(e^{-\Gamma t}). \quad \text{(A5)}$$

In particular, in the case $\gamma_1=\gamma_2$ and $R_1=R_2=\frac{1}{2}$ we obtain that the probe absorption decreases according to the same exponential low $\alpha\propto\exp(-\gamma t)$. Another result following from Eq. (A5) is that for the set of parameters for which the condition

$$\Omega_c^2R_1\gg\Omega_p^2R_2$$

is satisfied, the absorption of the probe field is replaced by its amplification as a result of the Raman scattering of the coupling field.

[1] S.E. Harris, J.E. Field, and A. Imamoğlu, Phys. Rev. Lett. **64**, 1107 (1990); K.J. Boller, A. Imamoğlu, and S.E. Harris, *ibid.* **66**, 2593 (1991); for a recent review, see S.E. Harris, Phys. Today **50**(7), 36 (1997).

[2] O.A. Kocharovskaya and Ya.I. Khanin, Pis'ma Zh. Éksp. Teor. Fiz. **48**, 581 (1988) [JETP Lett. **48**, 630 (1988)]; S.E. Harris, Phys. Rev. Lett. **62**, 1033 (1989); A. Imamoğlu and S.E. Harris, Opt. Lett. **14**, 1344 (1989); M.O. Scully, S-Y. Zhu, and A. Gavridiles, Phys. Rev. Lett. **62**, 2813 (1989).

[3] A.S. Zibrov, M.D. Lukin, D.E. Nikonov, L. Hollberg, M.O. Scully, V.L. Velichansky, and H.G. Robinson, Phys. Rev. Lett. **75**, 1499 (1995); G.G. Padmabandu, G.R. Welch, I.N. Shubin, E.S. Fry, D.E. Nikonov, M.D. Lukin, and M.O. Scully, *ibid.* **76**, 2053 (1996).

[4] S.E. Harris, Phys. Rev. Lett. **70**, 552 (1993); J.H. Eberly, M.L. Pons, and H.R. Haq, *ibid.* **72**, 56 (1994).

[5] M.O. Scully, Phys. Rev. Lett. **67**, 1855 (1991); M.O. Scully and M. Fleischhauer, *ibid.* **69**, 1360 (1992); A.S. Zibrov, M.D. Lukin, L. Hollberg, D.E. Nikonov, M.O. Scully, H.G. Robinson, and V.L. Velichansky, *ibid.* **76**, 3935 (1996).

[6] P.R. Hemmer, D.P. Katz, J. Donoghue, M. Cronin-Golomb, M.S. Shahriar, and P. Kumar, Opt. Lett. **20**, 982 (1995); M.D. Lukin, M. Fleischhauer, A.S. Zibrov, H.G. Robinson, V.L. Velichansky, L. Hollberg, and M.O. Scully, Phys. Rev. Lett. **79**, 2959 (1997).

[7] E. Arimondo, in *Progress in Optics*, edited by E. Wolf (Elsevier Science, Amsterdam, 1996), Vol. 35, p. 257.

[8] L.V. Hau, S.E. Harris, Z. Dutton, and C.H. Behroozi, Nature (London) **397**, 594 (1999); S.E. Harris and L.V. Hau, Phys. Rev. Lett. **82**, 4611 (1999).

[9] M.M. Kash, V.A. Sautenkov, A.S. Zibrov, L. Hollberg, G.R. Welch, M.D. Lukin, Yu. Rostovtsev, E.S. Fry, and M.O. Scully, Phys. Rev. Lett. **82**, 5229 (1999).

[10] Y.Q. Li and M. Xiao, Opt. Lett. **20**, 1489 (1995); Y. Zhu, Phys. Rev. A **55**, 4568 (1997).

[11] H.X. Chen, A.V. Durrant, J.P. Marangos, and J.A. Vaccaro Phys. Rev. A **58**, 1545 (1998).

[12] S. Brandt, A. Nagel, R. Wynands, and D. Meschede, Phys. Rev. A **56**, R1063 (1997).

[13] F. Renzoni, W. Maichen, L. Windholz, and E. Arimondo, Phys. Rev. A **55**, 3710 (1997); E.A. Korsunsky, W. Maichen, and L. Windholz, *ibid.* **56**, 3908 (1997).

[14] A. Izmailov, Opt. Spektrosk. **74**, 41 (1993) [Opt. Spectrosc. **74**, 25 (1993)].

[15] B. Zambon and G. Nienhuis, Opt. Commun. **143**, 308 (1997).

[16] S. Briaudeau, D. Bloch, and M. Ducloy, Europhys. Lett. **35**, 337 (1996); S. Briaudeau, D. Bloch, and M. Ducloy, Phys. Rev. A **59**, 3723 (1999).